Wavelength, power and pulse duration influence on spatial soliton formation in AlGaAs

V. Coda, R.D. Swain, H. Maillotte, G. Salamo, M. Chauvet

To be published in Optics Communication 2005

Wavelength, power and pulse duration influence on spatial soliton formation in AlGaAs

Virginie Coda [a,*], Ryan D. Swain [b], Hervé Maillotte [a], Gregory J. Salamo [b], Mathieu Chauvet [a]

[a] *Institut FEMTO-ST, UMR CNRS/Université de, Franche-Comté, Département d'Optique, 16 route de Gray, 25030 Besançon cedex, France*

[b] *Department of Physics, University of Arkansas, Fayetteville, Arkansas 72701, USA*

Received 9 December 2004; received in revised form 21 February 2005; accepted 22 February 2005

Abstract

This work presents the dependence of spatial soliton formation in AlGaAs slab waveguide versus significant parameters such as wavelength, light power, and pulse duration. Comparison between theory and experiments reveals the importance of multiphoton absorption to understand the soliton behavior. Experimental measurements establish some limits of soliton formation such as usable wavelengths and pulse durations.

PACS: 42.65.Tg; 42.65.Jx

Keywords: Nonlinear optics; Spatial solitons; Nonlinear absorption; Semiconductors; Kerr effect

1. Introduction

In materials that exhibit optical Kerr effect, for which the nonlinear index change is proportional to the light irradiance, optical fields localized in space or time can self-trap due to an optically induced positive index change [1]. If the nonlinear effect exactly balances diffraction or dispersion, respectively, spatial or temporal optical solitons exist, resulting in propagation without change of profile [2]. Solitons have received a great deal of attention due to their unique physical properties and a number of possible novel applications, such as long haul data transmission in optical fibers or light-induced reconfigurable waveguide structures [3]. One of the main reasons for the interest in solitons is their remarkable stability, which leads to a particle-like behavior [4,5].

* Corresponding author. Tel.: +33381666230; fax: +33381666423.
E-mail address: virginie.coda@univ-fcomte.fr (V. Coda).

To be published in Optics Communication 2005

Since the early nineties, much attention has focused on the use of semiconductors for realizing nonlinear integrated optical devices [6,7]. In particular, AlGaAs operated below the half-band gap spectral region has an almost ideal Kerr nonlinearity [8]. Its nonlinear refractive coefficient, n_2 is two order of magnitude greater than in silica and the absorption is low. In addition, the mature semiconductor fabrication technology available allows low-loss integrated optical component fabrication. Many publications deal with spatial solitons in AlGaAs [9–11]. Other works present this material's two- and three-photon absorption (2PA and 3PA) coefficients and show the implications for all optical switching and spatial solitons [8,12]. However, to the best of our knowledge, no direct implications of the multiple photon absorption (MPA) on solitons have been experimentally characterized in AlGaAs. In addition no studies of soliton behavior as a function of wavelength has been published.

In this paper we show the importance of nonlinear absorption on the soliton behavior as a function of light power. The influence of dispersion of MPA and Kerr effect versus wavelength is also explored. In addition we study the limits on soliton formation as a function of wavelength. Finally, we also discuss the influence of pulse duration on soliton propagation.

The paper is organized as follows. In Section 2 we introduce the basic equation and explicit the physical meaning of the different constituting terms. We present the experimental setup used in Section 3, along with typical results showing the remarkable stability of solitons in AlGaAs, in Section 4. We indeed propagate a soliton on 17 diffraction lengths. The soliton behavior versus wavelength is presented and discussed in Section 5 and the influence of MPA on soliton behavior versus power is analyzed in Section 6. The last section, deals with the influence of pulse duration on such solitons.

2. Theoretical background

The spatial soliton studied in this paper propagates in a planar waveguide. This guided configuration is necessary to obtain stable soliton in a Kerr medium. The beam propagates in the z-direction and is confined in the y-dimension by the fixed waveguide, diffraction can occur only in the third x-dimension. Model for the propagation of pulsed beam is based on the standard nonlinear Schrödinger equation which includes absorption

$$\frac{\partial E}{\partial z} - \frac{\mathrm{i}}{2k}\frac{\partial^2 E}{\partial x^2} + \frac{\alpha}{2}E - \mathrm{i}\frac{2\pi}{\lambda}n_2 I E = 0, \tag{1}$$

where E is the optical field related to the intensity through the relation: $I = 1/2c\epsilon_0 n|E|^2$. n_2 is the Kerr nonlinear coefficient, λ is the wavelength in free space, k is the propagation constant in the medium whose average refraction index is n. The total absorption α is given by

$$\alpha = \alpha_0 + \alpha_2 I + \alpha_3 I^2, \tag{2}$$

where α_0 is the linear absorption, α_2 is the 2PA coefficient and α_3 is the 3PA coefficient. Eq. (1) is numerically solved using the Split Step Fourier method, where the temporal shape of the beam is included. Absorption coefficient and n_2 values are extracted from reference [8].

3. Experimental setup

The semiconductor waveguides used in the experiments were grown by molecular beam epitaxy. Two different structures have been used. The structure of the first waveguide (WG1) consists of a 1-μm-thick guiding layer of $Al_{0.21}Ga_{0.79}As$, a 3-μm-thick lower cladding region and a 1-μm-thick upper cladding region of $Al_{0.3}Ga_{0.7}As$ deposited on a GaAs wafer. It was cleaved to give a 12-mm-long waveguide. The structure of the second waveguide (WG2) consists of a 1.5-μm-thick guiding layer of $Al_{0.24}Ga_{0.76}As$, sandwiched between two claddings similar than the first waveguide. This waveguide is 14-mm long.

Three different laser sources have been used: two optical parametric systems continuously tunable in the near-infrared region, delivering either femtosecond or picosecond pulses, and a 1.53-μm laser providing nanosecond pulses. The femtosecond system is an optical parametric amplifier (OPA) pumped by a CW-titanium:sapphire. The

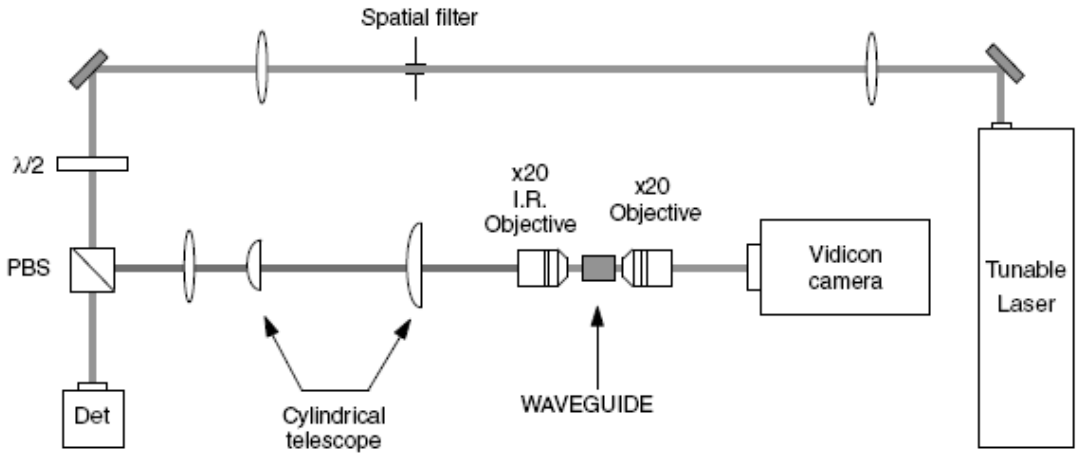

Fig. 1. Optical setup. $\lambda/2$ = half-wave plate, PBS = Polarizing beam splitter, Det = detector.

OPA repetition rate is 250 kHz. This system delivers 60-fs pulses with a typical energy of 300 nJ. We stretched the pulses in order to obtain a duration of 300-fs pulse using a two-prism system and a slit. The second system used is a picosecond system, which consist in an optical parametric generator pumped by a mode-locked Nd:YAG laser. It provides 20-ps long pulses at a repetition rate of 10 Hz, with an energy of about 100 μJ per pulse. Spatial filtering is necessary to improve the beam shape. The last source tested is a microchip laser delivering nanosecond pulses of 5 μJ at 1.53 μm.

A scheme of the experimental setup is represented in Fig. 1. For all setups, the beam was elliptically shaped using a set of cylindrical lenses before it was launched in the slab waveguide using a 20× microscope objective. Detection was made with a vidicon camera.

4. Stability of solitons

A remarkable result obtained with waveguide WG1 for a 30-ps pulse duration at 1480 nm, is shown in Fig. 2. A strongly focused input beam (6 μm HWHM) was launched at the entrance face of the waveguide as shown in Fig. 2(a). At low intensity, in the linear regime, the image at the exit face of the sample (Fig. 2(b)) depicts a strongly diffracted beam in accordance with the 17-diffraction-length long sample. As we increased the injected beam intensity, diffraction is partially balanced by the Kerr effect. At the proper beam power, a similar beam width is present at the entrance and at the exit face of the sample, a spatial soliton is formed (Fig. 2(c)). The smooth beam profile is also an indication of soliton formation. Indeed, noise present in the input beam and created by waveguide imperfections, is rejected during soliton formation and propagation. For energy slightly higher than the soliton threshold the input face of the waveguide is damaged. We can conclude that this soliton size necessitates a beam power close to the limit that can support the material. We evaluate this intensity to be 4 GW/cm^2. As a consequence smaller solitons could not be formed in AlGaAs, at least at this pulse duration. Spatial soliton for such a long propagation distance had never been shown in this semiconductor. In next section we explore the soliton stability versus wavelength.

5. Influence of wavelength

In the literature, soliton experiments in AlGaAs have been mostly done at a fixed wavelength (1.55 μm), the influence of wavelength on soliton propagation has consequently never been reported. In this section, we report experimental results on self-focusing for wavelengths varying from 1480 to 1570 nm in 10-nm steps. The results are depicted in Fig. 3. The output profiles are presented after propagation in waveguide WG2, with

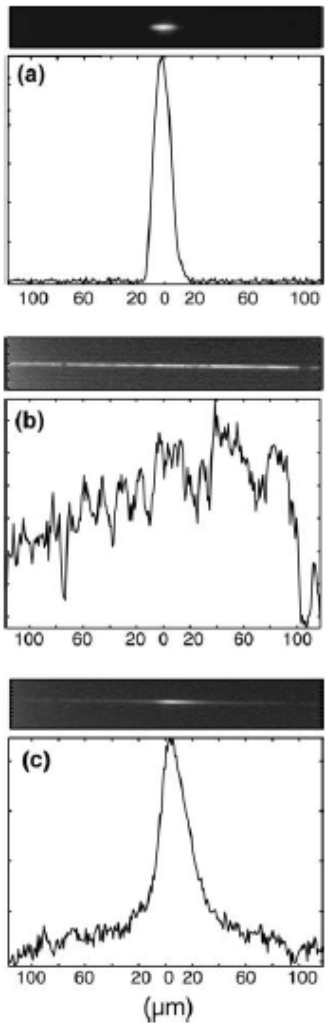

Fig. 2. Experimental images and profiles at the input (a) and output of the waveguide in linear regime (b) and soliton regime obtained after propagation on 17 diffraction lengths (c).

300-fs pulses. The beam width at the input is around 20 μm (HWHM) which corresponds to 3–4 diffraction lengths.

We note that the optimal wavelength is 1530 nm in accordance with the composition of this waveguide ($Al_{0.24}Ga_{0.76}As$). The bandgap of $Al_xGa_{1-x}As$ is indeed shifted toward short wavelengths when the concentration of aluminium increases, that is why the optimal wavelength is 1530 nm in our case instead of 1550 nm as reported for waveguides composed of 18% of aluminium [13]. At this optimal wavelength, we have a cleaned focused beam, with no local maximum on its sides. On the contrary, for the shortest wavelength we cannot obtain a clean focused beam without appearance of wings on both sides. For long wavelengths efficient self-focusing effect cannot be obtained even if we increase the injected power. For example at $\lambda = 1570$ nm in Fig. 3, a broad and noisy beam is present at the output face of the waveguide.

It has been shown that 2PA and Kerr effect coefficients are getting stronger for shorter wavelengths [8]. As a consequence of strong n_2, focusing remains present in our experiments, but 2PA adversely affects the focusing effect and gives rise to wings on both side of the central beam. This effect will be confirmed later using a numerical model. Experimentally, these side wings rise simultaneously with the clean central profile. The influence of 2PA will be discussed in more details in next section. For long wavelengths the weak self-focusing is mainly due to the Kerr effect that weakens for long wavelengths. Furthermore 3PA increases rapidly with wavelength and becomes non negligible [14]. We note that noise is removed from the profile only for short wavelengths when Kerr effect is strong which leads to a soliton-like behavior.

Dispersion of the nonlinear coefficients are key parameters in self-focusing behavior versus wavelength. We found that soliton propagation is effective for a range of 40 nm. In the following part we examine what happen at those optimal wavelengths when light power higher than the soliton threshold is injected in the waveguide.

6. Self-focusing behavior versus power

Self-focusing behavior as a function of beam power for 300-fs pulses is depicted in Fig. 4, where experiments and simulations are presented. A 14-μm-wide beam (HWHM) is injected at the entrance face of waveguide WG2 as shown in Fig. 4A(a). At low intensity, in the linear regime, the image at the exit face of the waveguide (Fig. 4A(b)) shows the diffracted beam in accordance with the 8-diffraction length long sample. The soliton regime is reached in Fig. 4A(c). If we increase the power above the soliton threshold, wings appear on each side of the beam. The wings become

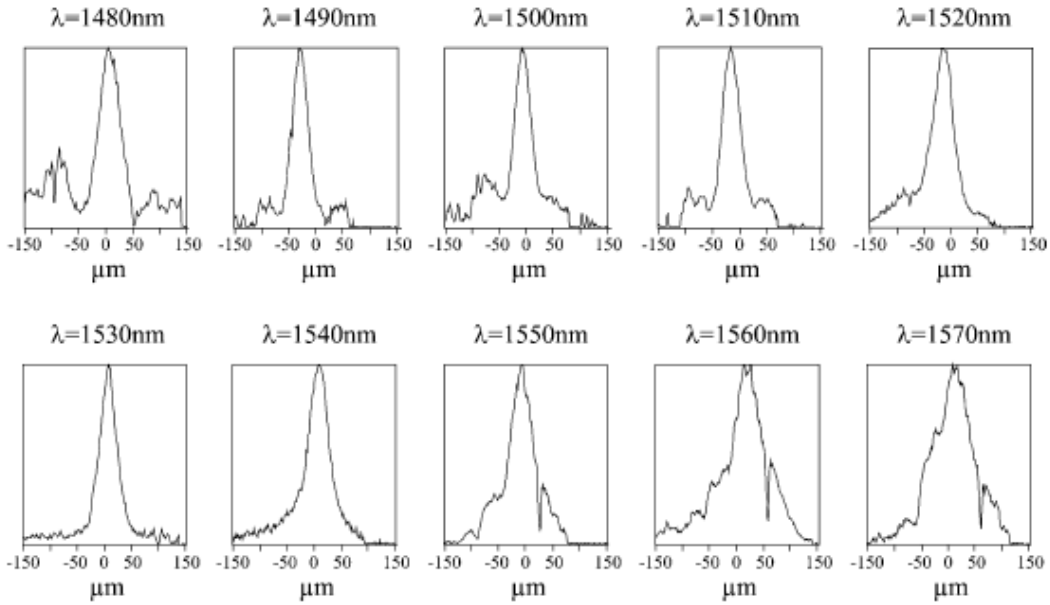

Fig. 3. Experimental output profiles showing the best "soliton" profile obtained as a function of wavelength.

more intense as we further raise the power (Fig. 4A(d)) and a 3-peak profile finally appears (Fig. 4A(e)). These 3 peaks have about the same width and they appear when the injected power is roughly three time the soliton power. For higher power the central peak becomes less intense than lateral ones as shown in Fig. 4A(f). Above this limit the transmitted power decays rapidly due to the nonlinear absorption, at the same time, the beam widens and the profile becomes chaotic probably due to modulational instability.

To show the fundamental influence of MPA on beam propagation at high power level [15], we have plotted in Fig. 5 the time averaged beam profile versus propagation length in absence and in the presence of nonlinear absorption. A beam propagation method has been applied to solve Eq. (1). Without nonlinear absorption we observe that after a strong focusing stage the beam splits in three peaks. These three peaks form a higher order soliton characterized by closely located peaks. For longer propagation length, the three peaks merge showing a recurrence effect. In the presence of MPA the three peaks are still obtained but they rapidly move away from each other and no recurrence is observed. The experimental behavior presented in Fig. 4 is in accordance with this last description.

MPA has consequently been included in the numerical results shown in Fig. 4 column B. A spatio-temporal representation showing the pulse reshaping is also presented. Because of nonlinear absorptions, at high power, the central part of the beam is highly absorbed and splits in two parts. At this point the intensity is low enough so that nonlinear absorption becomes negligible. In this case propagation is not affected anymore by the MPA and the beam evolves as if it was composed of two diverging solitons [16,17]. The front and the back of the pulse are not affected by MPA because of a lower power, and they self-focus to finally form the central peak superposition of two time shifted solitons. It consequently gives a 3-peak profile for the time integrated beam.

The intensity ratio between the lateral peaks and the central peak reaches a maximum for a given injected power (Fig. 4(f)). This maximum ratio depends on the amplitude of MPA and on the temporal shape of the pulse. For example if MPA is very high the strong absorption on the center of the temporal pulse prevents the spatial lateral peaks to reach the same intensity than the central

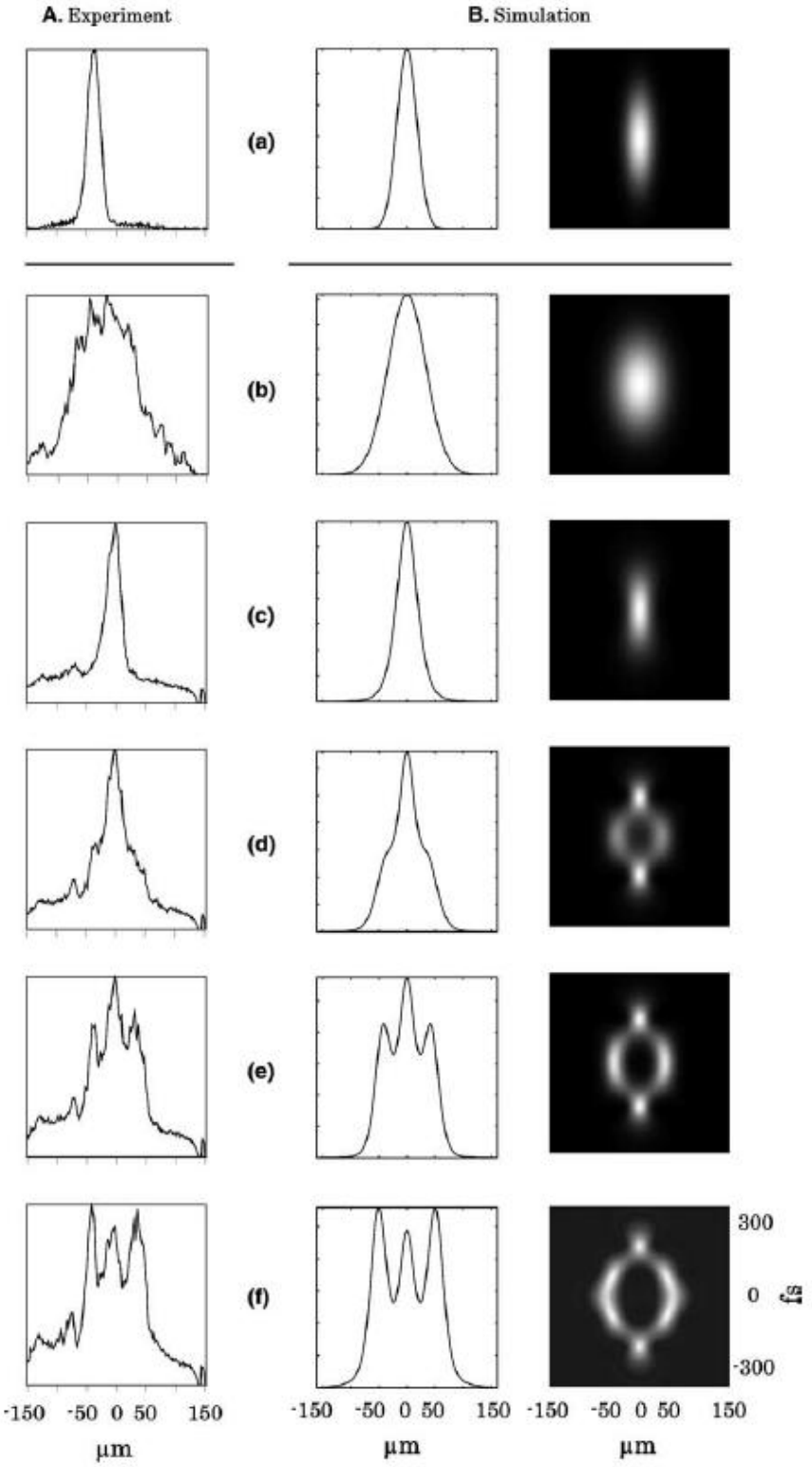

Fig. 4. Experimental profile (column A), numerical profile and spatio-temporal representation (column B) versus injected power. For $\lambda = 1520$ nm and 14-mm propagation length. Injected beam (a) and output beam in linear regime $P < P_{sol}$ (b), soliton regime $P = P_{sol}$ (where $I_0 = 0.5$ GW/cm^2, in theory) (c), $P = 2.2P_{sol}$ (d), $P = 2.7P_{sol}$ (e), $P = 3P_{sol}$ (f).

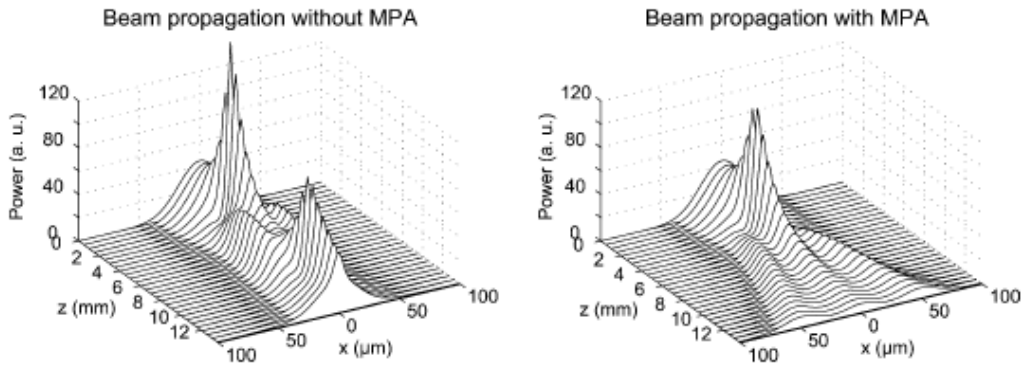

Fig. 5. Time-averaged beam evolution of an initially Gaussian beam versus propagation without and with MPA for an input intensity of three time the soliton intensity ($I_0 = 3I_{sol} = 1.6$ GW/cm^2 and $HWHM = 20$ μm). Material parameters used are $\lambda = 1.52$ μm, $n_2 = 1.75 \times 10^{-4}$ cm^2/GW, $\alpha_0 = 0.16$ cm^{-1}, $\alpha_2 = 0.45$ cm/GW and $\alpha_3 = 0.04$ cm^3/GW^2.

spatial peak and the behavior is then dominated by the back and front of the pulse. On the contrary if the temporal pulse shape is not gaussian, as taken in the numerical calculation, but with a flat top (super-gaussian), the lateral peaks will contain most of the energy. In this case the back and front of the pulse beam do not play a significant role. This situation is close to the case of a continuous wave. The extreme case is a continuous beam that would not produce a central peak at high power. In addition, our numerical beam calculations shows than 2PA and 3PA play a similar role on the spatial profile, They both give rise to a profile composed multiple peaks at high power.

We have shown that MPA plays a major role in self-focusing for intensity higher than the soliton threshold intensity. It particularly prevents higher order soliton and recurrence to occur in AlGaAs waveguide.

7. Influence of pulse duration

In the previous part some influence of the pulse shape has been shown. In this section we analyze the effect of pulse duration on soliton formation. Discrete pulse durations have been experimentally used. When using 60-fs pulses weak focusing effect is observed, not sufficient to spatially trap even wide beams. For high power transmissivity of the waveguide decreases rapidly preventing soliton regime to be reached. The rapid decay is due to both MPA and chromatic dispersion. Most of our experiments have been performed with 300-fs pulses for which optical damage of the AlGaAs does not occur even for the highest used intensities. For this pulse duration, we however suspect that dispersion still has an impact on soliton formation since narrow solitons cannot be formed despite sufficient light power. On the contrary, 30-ps pulses can generate very narrow solitons as shown in Section 2. For picosecond pulses we could expect the effect of carrier generation to induce defocusing [18,12], we however did not observe experimentally any influence of this effect on beam trapping. Finally, for 2.5-ns pulses, we observed that waveguide facet damage occurs before appearance of self-focusing. We suspect this damage to be due to thermal effects. Moreover for these long pulses the photo-generated free carriers induced by 2PA and 3PA would result in a strong adverse defocusing effect and we suspect that self-focusing would not be possible. The experiments lead us to conclude that the optimum pulse duration for soliton in AlGaAs is in the picosecond range.

8. Conclusion

We have demonstrated that Kerr self-focusing in AlGaAs can be obtained over a wide range of wavelength (about 70 nm) in the vicinity of 1550 nm. The soliton formation is however limited to a narrower range whose limits are due to 2-photon absorption on the short wavelength side and a weak Kerr effect associated with 3-photon

absorption for long wavelengths. Comparison between theory and experiments reveal that nonlinear absorptions cannot be neglected even at the optimal 1530 wavelength to fully understand beam self-focusing behavior as a function of power. The multi-photon absorption prevents higher order solitons to propagate in AlGaAs. At last, we observe that material chromatic dispersion imposes a minimum value for pulse duration while material damage threshold sets the maximum value. Pulses in the picosecond range gives the best results for spatial soliton formation. Finally we have shown than solitons can propagate over a long distance when optimum parameters are used. Stability has been observed over 17 diffraction lengths.

References

[1] R.Y. Chiao, E. Garmire, C.H. Townes, Phys. Rev. Lett. 13 (1964) 479–482.

[2] V.E. Zakharov, A.B. Shabat, Sov. Phys. JETP 34 (1972) 62–69.

[3] Y.S. Kivshar, G.P. Agrawal, Optical Solitons, Academic Press, 2003.

[4] C.R. Menyuk, J. Opt. Soc. Am. B 10 (1993) 1585–1591.

[5] N.J. Zabusky, M.D. Kruskal, Phys. Rev. Lett. 15 (1965) 240–243.

[6] K. Al-Hemyari, J.S. Aitchison, C.N. Ironside, G.T. Kennedy, R.S. Grant, W. Sibbet, Electron. Lett. 28 (1992) 1090–1092.

[7] J.S. Aitchison, A. Villeneuve, G.I. Stegeman, Opt. Lett. 18 (1993) 1153–1155.

[8] J.S. Aitchison, D.C. Hutchings, J.U. Kang, G.I. Stegeman, A. Villeneuve, IEEE J. Quantum Electron. 33 (1997) 341–348.

[9] J.S. Aitchison, K. Al-Hemyari, C.N. Ironside, R.S. Grant, W. Sibbett, Electron. Lett. 28 (1992) 1879–1880.

[10] J.U. Kang, J.S. Aitchison, G.I. Stegeman, N.N. Akhmediev, Opt. Quantum Electron. 30 (1998) 649–671.

[11] R.R. Malendevich, L. Friedrich, G.I. Stegeman, J.M. Soto-Crespo, N.N. Akhmediev, J.S. Aitchison, J. Opt. Soc. Am. B 19 (2002) 695–702.

[12] J.S. Aitchison, M.K. Oliver, E. Kapon, E. Colas, P.W.E. Smith, Appl. Phys. Lett. 56 (14) (1990) 1305–1307.

[13] S. Trillo, W. Torruellas, Spatial Solitons, Springer, Berlin, 2001. Chapter: One-dimensional spatial solitons in Kerr media, chapter by Y. Silberberg and G.I. Stegeman.

[14] J.U. Kang, A. Villeneuve, M. Sheik-Bahae, G.I. Stegeman, K. Al-Hemyari, J.S. Aitchison, C.N. Irondside, Appl. Phys. Lett. 65 (1994) 147–149.

[15] J.S. Aitchison, A.M. Wiener, Y. Silberberg, M.K. Oliver, J.L. Jackel, D.E. Leaird, E.M. Vogel, P.W.E. Smith, Opt. Lett. 15 (1990) 471–473.

[16] Y. Silberberg, Opt. Lett 15 (1990) 1005–1007.

[17] V.V. Afanasjev, J.S. Aitchison, Y.S. Kivshar, Opt. Commun. 116 (1995) 331–338.

[18] E.W. Van Stryland, H. Vanherzeele, M.A. Woodall, M.J. Soileau, A.L. Smirl, S. Guha, T.F. Boggess, Opt. Eng. 24 (4) (1985) 613–623.